RSC Advances

PAPER

View Article Online
View Journal | View Issue

Cite this: *RSC Adv.*, 2022, **12**, 4526

Archaeometric study of execution techniques of white Attic vases: the case of the Perseus crater in Agrigento†

Gabriella Chirco, *[ab] Monica de Cesare,*[a] Giacomo Chiari,[f] Sarah Maaß,[e] Maria Luisa Saladino [b] and Delia Francesca Chillura Martino [bcd]

Received 26th August 2021
Accepted 4th January 2022

DOI: 10.1039/d1ra06453c

rsc.li/rsc-advances

The white ground crater by the Phiale Painter (450–440 BC) exhibited in the "Pietro Griffo" Archaeological Museum in Agrigento (Italy) depicts two scenes from Perseus myth. The vase is of utmost importance to archaeologists because the figures are drawn on a white background with remarkable daintiness and attention to detail. Notwithstanding the white ground ceramics being well documented from an archaeological and historical point of view, doubts concerning the compositions of pigments and binders and the production technique are still unsolved. This kind of vase is a valuable rarity, the use of which is documented in elitist funeral rituals. The study aims to investigate the constituent materials and the execution technique of this magnificent crater. The investigation was carried out using non-destructive and non-invasive techniques *in situ*. Portable X-ray fluorescence and Fourier-transform total reflection infrared spectroscopy complemented the use of visible and ultraviolet light photography to get an overview and specific information on the vase. The XRF data were used to produce false colour maps showing the location of the various elements detected, using the program SmART_scan. The use of gypsum as the material for the white ground is an important result that deserves to be further investigated in similar vases.

Introduction

In ancient Greece white ground ceramics were used in burial and in sacred contexts and typically showed funeral related pictures either of the funerary rituals, of the deceased or mythological scenes.[1–3]

The interest of archaeologists toward Attic white ground ceramics is well documented,[4,5] while the archaeometric studies are limited. To our knowledge, only Meissner[6] and Berthold studied lekythoi.[7]

The white ground, common in lekythoi[8–10] was rarely applied to craters.

The Perseus crater is an Attic vase, painted by the Painter of the Phiale, whose work is dated back to 450–440 BC.[1] The vase was found in 1940 in the Contrada Pezzino's necropolis (Agrigento, Italy), and now it is exhibited in the archaeological museum "Pietro Griffo" in Agrigento. It is a precious example of vases painted using the white ground technique, a rarity compared with the more common red-figure ceramics. A white slip is applied to the entire vase, and the figures and patterns are drawn onto it, enabling the artist to contour figures with daintiness and paint with vibrant colours. The delicate painting on the crater (Fig. 1), probably a cinerary, illustrates the part of the Perseus and Andromeda myth, in which the hero sets free the princess immolated to a marine monster.

The iconography of the vase has been the focus of investigations, mainly concerning the side A inscription celebrating Euaion, Eschilo son's, widely known for many acclaims on vases. Perhaps, the inscription connects the vase to its context of use; in fact, the renowned tragedian Aeschylus died in Gela, Sicily, a few years earlier, in 456 BC. The inscription also led to an immediate association of the crater with theatre, as suggested by the represented mythical episode, made famous in those years by Sophocles' almost wholly lost tragedy.[1,11]

The vase shows a male figure resting his foot on a stone and holding two spears in his hand and a female figure tied to three

[a]*Dipartimento di Culture e Società Università degli Studi di Palermo, Viale delle Scienze ed.15, Cap 90128, Palermo, Italy. E-mail: monica.decesare@unipa.it*

[b]*Dipartimento Scienze e Tecnologie Biologiche, Chimiche e Farmaceutiche – STEBICEF, Università di Palermo, Viale delle Scienze pad.17, Palermo-90128, Italy. E-mail: gabriella.chirco@unipa.it*

[c]*ATeN Center-Laboratorio di Caratterizzazione della Struttura Atomico-Molecolare, Università di Palermo, Via F. Marini 14, Palermo I-90128, Italy*

[d]*Consorzio Interuniversitario Nazionale per la Scienza e Tecnologia dei Materiali (INSTM) - UdR of Palermo, Università di Palermo, Viale delle Scienze pad.17, Palermo 90128, Italy*

[e]*Department of Natural Sciences, University of Applied Sciences Bonn-Rhein-Sieg, von Liebig-Str. 20, 53359 Rheinbach, Germany*

[f]*Getty Conservation Institute (Retired), S. Tommaso 29, 10121 Torino, Italy*

† Electronic supplementary information (ESI) available. See DOI: 10.1039/d1ra06453c

Fig. 1 The Perseus crater exhibited in the "Pietro Griffo" Archaeological Museum in Agrigento. Left, side (A) – Perseus and Andromeda; right, side (B) – Aphrodite and Cassiopeia.

posts. On side A the inscription above the male's head makes it easy to identify him as Perseus, and the female figure is identified as Andromeda.

Usually, the figures on side B have been connected to the scene on side A, although their identification is complicated by the lack of inscription on this side. The two women have been interpreted as the goddess Aphrodite in the act of instilling in Perseus love for the chained girl, and the queen Cassiopeia (Andromeda's mother and wife of the king of Ethiopia Cepheus), responsible for the fate of her daughter. Cassiopeia claimed to be more charming than the Nereids. For this reason, the fierce god Poseidon sent a sea monster to which King Cepheus was forced to sacrifice his daughter Andromeda.

The vase is a singular artefact of great value; the pictorial technique attributes to colour a symbolic value, as recently proposed by de Cesare.[1] The red of Aphrodite's dress evokes desire, seduction, eroticism, possessed by both the goddess of love and by Andromeda, with whom Perseus fell in love. On the contrary, the black of Cassiopeia's cloak anticipates the mourning for her daughter reached by the sea monster if Perseus had not intervened.

The vase is also extraordinary for its use in a funerary ritual (cremation in a crater), probably connected with eschatological beliefs related to the sphere of the Dionysian cult. The figurative themes confer a funerary and salvific meaning: the crater evokes Dionysus (the god of wine mixed with water inside the crater, accordingly to Greece custom) transformation and rebirth.

We undertook an archaeometry survey aimed at shedding light on the pictorial technique.[1] The preliminary results indicated the use of earths as pigments and evidenced organic materials as a probable consequence of conservative interventions. Notwithstanding, information about the pictorial technique were not conclusive. For this reason, we extended the investigation on the entire vase surface through X-ray Fluorescence (XRF), total reflection Fourier-transform infrared spectroscopy (TR-FTIR) complemented with visible and ultraviolet light photography to get an overview and specific information on the slip composition and on the pictorial technique. The archaeometry survey was designed to account for some technical issues connected with the preciousness of the artefact. Indeed, portable, noninvasive, and non-destructive techniques were selected to be applied directly *in situ*, thus avoiding all the required bureaucracy for moving the vase from the museum site.

The XRF data were used to produce false colour maps showing the location of the various elements detected, using the program SmART_scan.[12–14] This software is a valid alternative, although not as accurate, to the XRF scanners that recently came in use.[42] The main difference is that the XRF scanners collect a massive amount of data. At the same time, SmART_scan only uses a limited number of measured points, accurately selected, representing the various colours of interest.

Experimental part

Instrumentation

Photos were acquired under visible and UV light (Wood E27 lamp with a power of 160 W) by a NIKON D500 camera equipped with an 18–55 mm photographic lens.

The microscopy images were taken with a DigiMicro USB microscope 1.3 Mpix with Digivision digital camera.

Energy-dispersive X-ray fluorescence analysis was carried out using a portable spectrometer Tracer III SD Bruker AXS. The detector is a silicon drift X-Flash SDD detector with Peltier cooling system and 3–4 mm diameter spot. The source is a Rhodium Target X-ray tube operating at 40 kV and 11 mA. Four different filters allow a good sensitivity both at lower and higher energies (up to barium K – lines). Each spectrum was

acquired for 30 s. The energy resolution of the spectrometer is 150 eV at 5.9 keV. Measurements were acquired without the need for reduced pressure in the head of the instrument. The window of the instrument was placed in contact with the sample surface. S1PXRF® Software was used for data acquisition. The spectra interpretation was performed using X-ray software (ARTAX®). To quantify the previously identified elements, the spectra were processed with the Origin® 8.51 software, where the peaks' intensity and area were estimated using the multiple peak fit function, utilizing Gaussian functions.

A portable Bruker ALPHA spectrometer was used to record the FTIR spectra. It comprises a MIR lamp source, a KBr beam splitter, a Rocksolid® oscillating interferometer and a DTGS detector (Deuterated Triglycine Sulfate). These allowed the collection of spectra in the range 5900 to 360 cm^{-1} with 4 cm^{-1} resolution. The acquisition time used for data collection in the present work was 60 s. The operations were performed using the software OPUS 7.5®. The spot size on the investigated sample was about 4 mm^2. The instrument was kept perpendicular to the sample surface (typical geometry) by a mechanical arm. The probe to surface distance is fixed at about 5 mm by a spacer. Due to the combined diffuse and specular components, the total reflectivity, R, was collected over 400 scansions using the spectrum from a gold mirror plate for background correction. Spectra were expressed as a function of pseudo-absorbance A' where $A' = \log(1/R)$. The elemental maps were obtained using the program SmART_scan, which used 11 XRF measurements for side A and 19 measurements for side B (Fig. 2). For each measured point, the program uses the X,Y position coordinates, the RGB colour values and the element's counts obtained by XRF. The chemistry of the point presenting the minimal Euclidean distance in the multi-dimensional space is assigned to each unknown point. The abundance of each element on each point of the whole vase is then used to draw the maps, according to a colour scale that can be chosen at will. Some selected maps are shown. For all of them, the black colour represents the maximum abundance.

Sampling

Measurements were carried out on different coloured areas as indicated in Fig. 2. The full description of each measurement point is deposited as ESI (Table SI1†). Each measurement is identified by a string of letters (A or B, relative to the vase's side, X for XRF and R for TR-FTIR spectroscopy) and sequential numbers.

Results and data elaboration

The visual inspection of the crater confirms the quite good conservation state of the vase; it does not show lesions or gluing, only some colour layers are abraded, but it is possible to appreciate the original colours from residues of the picture.

The painting layers on the white slip and the engravings defining some anatomical details are appreciable under grazing incidence light (Fig. SI1†). Craquelures and abrasions show the sequence of the painting layers.

From UV photos (Fig. 3 and SI4†), the white areas emit a diffuse blue fluorescence, more intense in some areas.

The black, red, and brown hatching do not fluoresce, thus suggesting the use of oxides or ochre.[15] The UV images do not evidence retouched areas.

An XRF spectrum, as an example, is shown in Fig. 4, where the attribution of emission energy to each element is also reported. All spectra are shown in Fig. SI5–SI11.† The elements were identified by using the ARTAX® software, and the contribution to elements counts of the inner walls of the instrument, environment, source, and detector were accounted for accordingly to previous work.[16] The identified majority elements are

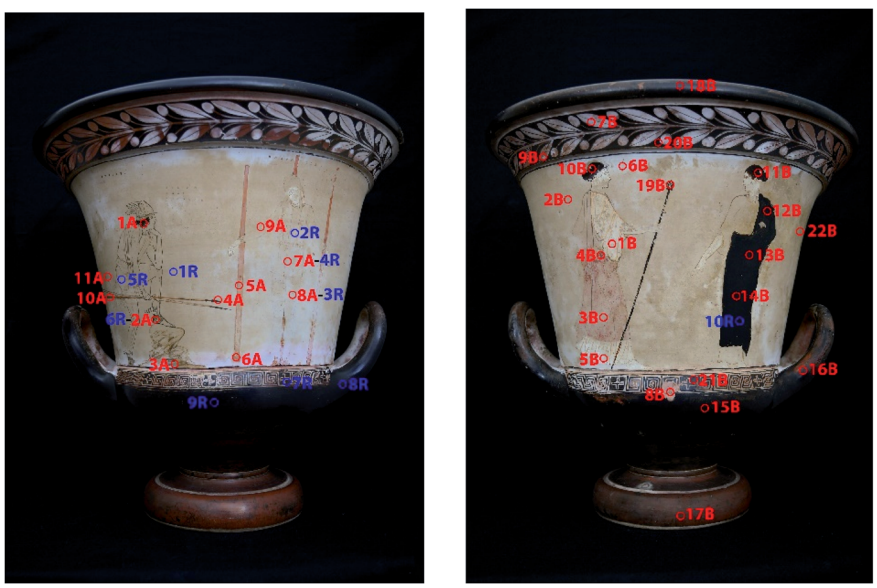

Fig. 2 Map of acquisition points XRF in red and FTIR in blue. Left, side (A); right, side (B).

Fig. 3 Detail of Aphrodite (left) and Perseus (right) under visible and ultraviolet light.

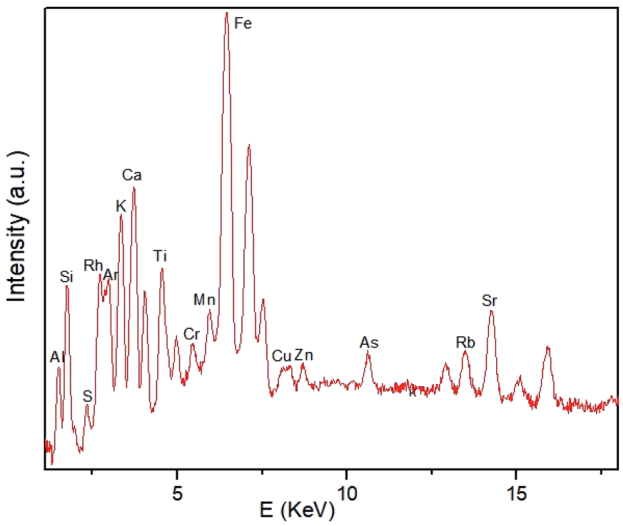

Fig. 4 Intensity (logarithm scale, arbitrary units – a.u.) *vs.* energy (keV) for the XRF spectrum for the point 14B. Attribution of emitting elements is indicated. Rh and Ar are from the source and the environment respectively, accordingly to previous work.[16]

calcium and iron. The minority elements Al, Si, S, K, Ti, Cr, Mn, Cu, Zn, As, Rb and Sr were detected in all spectra.

Accordingly to a previous work,[16] the composition for each investigated area was evaluated based on the neat peak area (Table SI1†), while the compound nature was obtained from the peak area ratio among predominant and discriminant elements.

The ratios between calcium and iron and between iron and manganese minority element, depend on hues (Table 1). The variability of calcium and iron is high. From Tables 1 and SI1,† it becomes apparent that all black points have a higher concentration of iron and a lower concentration of calcium, *i.e.*, low calcium/iron ratio, unless the probed area comprehends a portion of the slip (points 4A and 19B). The iron/manganese ratio is generally higher on black than on white points, thus suggesting an iron oxide as black pigment.

The red areas show a high iron content, coherently with the use of red ochre.

The XRF intensity for arsenic is appreciably higher in deep black regions than in all other points. This finding is confirmed by the SmART_scan map shown in Fig. 5B. All elements other than Ca, Fe and Sr show slight variation in the peak areas, as reported in Table SI1.† The values for Sr are relatively similar in most spectra, except in point 1A. The SmART_scan map for strontium evidenced a higher intensity within the white coloured areas corresponding to the himation of Aphrodite and the Cassiopeia's arm (Fig. 5C). The K peak area appears to be higher in all black spectra except in point 16B.

The TR-FTIR spectra were analysed by identifying single bands based on the literature database for organic compounds and some minerals (Table SI2, Fig. SI12 and SI13†).

All TR-FTIR spectra acquired on white areas (1R, 2R, 3R, 4R, 5R, 6R) show bands characteristic of an organic compound. The band at 3323 cm^{-1} (N–H stretching), the band at 1640 cm^{-1} (amide I) and the band at 1550 cm^{-1} (N–H bending, amide II) are due to a proteinaceous compound.[17,18] The C=O stretching of an ester at *ca.* 1740 cm^{-1},[17,18] as well as the C–H stretching at *ca.* 2900 cm^{-1}, and the scissoring (1470 cm^{-1}) of aliphatic CH_2, and bending of ester CH_2 (1375 cm^{-1}) are typical of wax.

The band at 5170 cm^{-1} may be attributed to crystal water in sulphates. The broadband ranging from 3750 to 3000 cm^{-1} can be attributed to OH stretching in silicates or sulphates.

The SO_4 overtones at *ca.* 2540 and 1990 cm^{-1}, S=O stretching at *ca.* 1375 cm^{-1}, the symmetric and asymmetric SO_4 stretching at *ca.* 1170 and 1085 cm^{-1}, respectively,[19] the SO_4 bending *ca.* 680 cm^{-1}, are characteristics of calcium sulphate.[20]

The Si–O–Si asymmetric and symmetric stretching at *ca.* 1046, 960, 826 and 758 cm^{-1}, and the Al–O–Si bending at *ca.* 550 cm^{-1} are coherent with aluminosilicates and were identified by comparison with the spectra from lisa.chem databases.[21,22]

Discussion

The bluish ultraviolet fluorescence observed could indicate calcite or gypsum, used for the white slip, or resin as a protective due to a conservative intervention. However, the use of resins has been excluded by TR-FTIR findings.

Table 1 Acquisition point, ratio between Ca and Fe and between Mn and Fe

Point	Ca/Fe	Fe/Mn
Clay		
8B	0.114	0.009
22B	0.706	0.017
Black on white		
1A	0.351	0.012
4A	0.363	0.050
10B	0.117	0.007
11B	0.041	0.006
12B	0.076	0.007
13B	0.050	0.007
14B	0.068	0.007
20B	0.134	0.008
19B	0.351	0.013
21B	0.087	0.008
Black		
15B	0.034	0.006
16B	0.279	0.007
17B	0.067	0.007
18B	0.038	0.007
Brown		
2A	0.400	0.018
3A	0.374	0.025
White yellowish slip		
2B	0.483	0.015
7A	0.636	0.018
8A	0.637	0.015
9A	0.463	0.015
11A	0.659	0.018
White slip		
6B	0.696	0.015
7B	0.233	0.011
9B	0.141	0.009
White		
1B	0.256	0.012
5B	0.392	0.012
Red		
3B	0.549	0.014
4B	0.485	0.013
Orange		
5A	0.522	0.015
6A	0.729	0.015
10A	0.485	0.017

The different hue of blue fluorescence could be interpreted as indicative of the heterogeneous thickness of pigments and protective (wax) and its ageing, due to physical abrasion and reactions with the environment.

The visual inspection and photographs (Fig. SI13 and SI14†) evidenced some micro-gaps and abrasions, which allowed to see the reddish colour of the ceramic's body. The XRF data in those regions correspond to elements typical of the minerals contained in the vase body. All spectra acquired on these points have comparatively larger iron peaks suggesting the presence of iron minerals, probably oxidized to hematite (Fe_2O_3) during the firing process, in accordance with the observed reddish colour. The iron content is coherent with the known raw material, goethite (FeO(OH)) and illite ($(K,H_3O)(Al,Mg,Fe)_2(Si,Al)_4O_{10}[(OH)_2,(H_2O)]$) rich clay used to produce Attic vases.[9,23–26] TR-FTIR spectra show the bands characteristics of silicate minerals fired at temperatures between 700 and 900 °C.[24,25,27,28] In particular, the distinctive bands at 3650 and 826 cm^{-1} suggest the presence of chlorite ($(Mg,Fe^{2+},Fe^{3+},Mn,Al)_{12}[(Si,Al)_8O_{20}](OH)_{16}$)[22,29,30] that could be assumed as an indicator of the firing temperature.[31,32]

The black gloss area in the top rim, the foot and the handle appear thick, smooth, and shiny, thus suggesting that it results from the firing process typical of black figure Attic vases. The stratigraphy of the decoration was observed from macrophotography (Fig. 6 and SI16†).

The white layer on the wreath was painted first on the ceramic. Then, the leaves were outlined with black pigment and defined with ticker lines (see Fig. SI17†). On the rim and foot, the black pigments were directly applied on ceramic.

The XRF data showed that the entire vase contains large amounts of calcium, partly attributed to the white ground and the clay minerals. The white slip could contain calcium carbonate, kaolinite or calcium sulphates.[33] Maps obtained by SmART_scan imposing that calcium and sulphur be simultaneously present (Fig. 5D) indicate the distribution of gypsum covering the entire ground. The white parts in Fig. 5D are due to the Ca and S fluorescence absorption by the pigments overlaying it, essentially iron oxides, as evidenced by the iron distribution map (Fig. 5E). The sulphur[34] and strontium data (Fig. SI3A†) could indicate gypsum containing naturally occurring impurities of strontium sulphate (celestine).[35–37]

TR-FTIR spectra have excluded the eventual presence of kaolinite or calcium carbonate while the contribution of crystal water in sulphates and the OH stretching strengthen the XRF evidence about gypsum presence. This issue has been debated in literature with no straightforward conclusion about the composition of the slip layer. Meissner *et al.*,[6] who investigated five samples taken from white ground ceramic evidenced, for three of these, a clayey layer superimposed on the ceramic body in line with the most widespread and known vascular technique, while for the two remaining samples, they detected a layer of gypsum. Berthold *et al.*[7] confirmed the presence of gypsum on one lekythos. The water band and the broad OH stretching in all spectra acquired on white areas can be attributed to gypsum.[18,19] Furthermore, the OH bending vibration of water at 1685 cm^{-1} observed in all spectra is attributed to structural water in gypsum.[38] The presence of gypsum on the vase suggests that it was applied subsequently to the vase firing[16,23,26] like for the Attic lekythos studied by Berthold.[7]

To draw the figures, the inscription, and the decoration overlying the white background, the only pigments used were black, white and red. The leaves and the details were realized on the top rim by contouring the motif directly on the white background (Fig. SI17†). The figures were realized by engraving upon the preparation layer, probably with a thin metal tip or

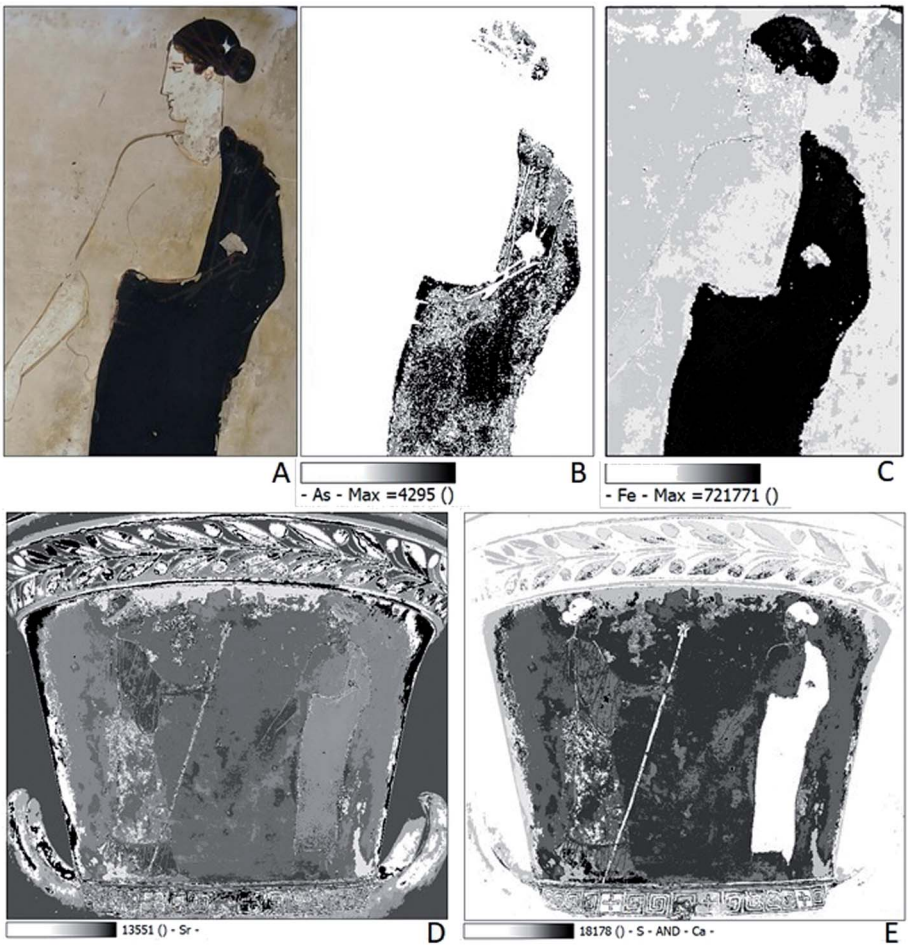

Fig. 5 (A) Detail of Cassiopeia under visible light; (B) map of arsenic; (C) map of iron; (D) map of strontium; (E) map of calcium and sulphur.

Fig. 6 Raking light detail of Aphrodite's face where painted layers succession, thickness of the white pigment and his craquelure are visible.

blade, as shown in the photographs in grazing light (see, for example, Andromeda legs, Fig. SI2†).

The images also clearly show a white layer on the white ground on the female hands, face and neck, and the white parts of Aphrodite himation, to enhance these details. This white layer appears thick, with cracks and whiter than the intact ground underneath (see Fig. 3A, 6 and SI16†). The XRF spectra of these regions show higher sulphur and calcium content, thus suggesting that the additional white layer is mainly composed of gypsum (Fig. 5D). The whiter colouration could be caused by the higher thickness and possibly density of the paint.

The red colour used only for Aphrodite peplum on side B appears severely abraded. The red pigment is most likely red ochre, one of the favoured red pigments of the Greeks.[10,39] The appearance of the red coloured areas suggests that the pigment was applied after firing the vase because the layer appears very thin, the colour is not evenly distributed, and the surface appears dull and powdery. Upon firing, the surface would be shiny, and the colour would likely be a thicker, more solid layer with a homogenous colouration and a deeper red colour.[10]

To make the subject three-dimensional the coloured areas are defined with black or brown-orange outlines of different intensities and shades. On the side A, all the contour lines of Perseus are drawn using an iron bases pigment (Fig. 7B). These, unlike the large black areas on foot, the rim, and the handles, were applied above the others colours and were not fired.

It is possible to see the brushstrokes in the thicker white layer under the DigiMicro microscope (see Fig. SI18 and SI19†). The absence of colour diffusion suggests that they were applied

Fig. 7 Maps of Perseus (side a) (A) detail of Perseus under visible light; (B) iron; (C) manganese.

when the white paint was dry. The brown-orange details appear to be very thin and almost transparent. The brown pigment, which was used to outline the women, and the Perseus contours under his clothing, is most likely composed of a mixture of iron and manganese oxides (Fig. 7C and SI3B†). However, due to the subtle lines and the thin, almost transparent layer of paint, the XRF spectra acquired in these areas do not differ much from the other spectra.[40] The black coloured areas (Cassiopeia's dress, geometrical decorations on the bottom of the vase, Perseus, Aphrodite, and Cassiopeia hair) were painted on the white slip after firing. The high iron content suggests that the pigment was most likely magnetite.[7] It should be noticed that arsenic is present in all areas investigated. Its X-ray fluorescence intensity is appreciably higher on the Cassiopeia's dress, suggesting the use of a ferrous mineral naturally enriched in arsenic compound.[41] The advantage of the use of SmART_scan is to map elements present in small amounts or in traces, whose interpretation is difficult when just considering the XRF data. This advantage clearly emerges when focus on the dress and the hair of Cassiopeia on the side B. It may be surprising that the dress is rendered with a dull, uniform black colour, in contrast with the refined drawings of the other figures.

When mapping iron (Fig. 8B) the difference in the XRF intensity is not enough to be perceived, and the map of a minor element is needed to evidence the lighter lines. The titanium map (Fig. 8C) generates a negative image that shows lines on the dress representing drapery, making the drawing much more sophisticated and naturalistic. The same for the hair dress. These lines are just a nuance lighter than the colour of the dress and were probably perceivable on the fresh original. Coherently, similar maps are obtained by combining titanium with aluminium and silicon (Fig. 8D). These findings suggest the use of a mixture of magnetite and alumino-silicate to render the bright and deep black of the Cassiopeia's himation on which the lighter lines were realized with magnetite only pigment.

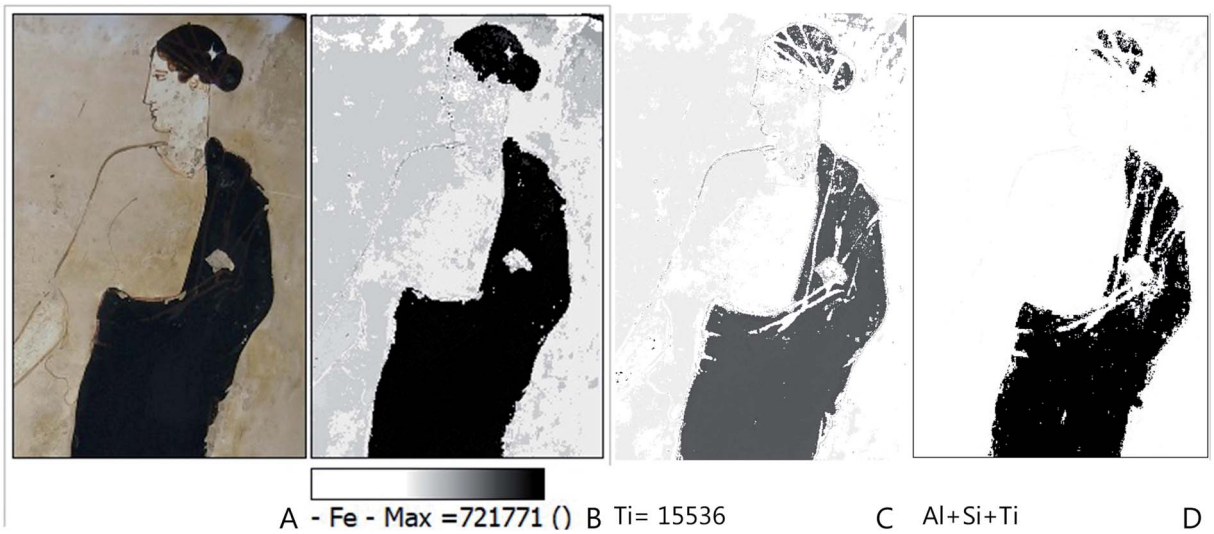

Fig. 8 Maps of Cassiopeia, (A) detail under visible light; (B) map of iron; (C) map of titanium; (D) map of Al, Si, and Ti.

The organic compounds contributions in all TR-FTIR spectra indicate a protein-based organic compound (NH– stretching, C═O stretching, and amide bands), thus suggesting the realization of the decorations and figures on the vase body *via* tempera painting. The contemporary presence of wax contributions (CH– stretching and C═O stretching of ester) could indicate a later intervention focused on its preservations or confer shine to the surface.

Conclusions

The Perseus' crater investigation evidenced the realization technique of this rare example of white ground ceramic.

The vase was fired after completing the decoration on the top rim, the foot, and the handle. The firing temperatures, evinced by the presence of new formation compounds, was between 700 and 900 °C, as known for Attic vases.

After firing, the vase was first covered by a white slip composed of gypsum.

The iconography was realized by engraving the figures by a blade or a metal tip and contoured with black or brown lines. The evidence of a protein-based compound suggests that the painting technique was tempera. The pigments that were used are gypsum for white, iron oxides rich in manganese oxide for black and brown, and red ochre for red and orange. The black painting contains arsenic and could be indicative of the provenance of the pigment.

The artist realized some details in the figures by superimposing the painting to the already coloured area.

The attained indications about the composition of the white ground suggesting the use of gypsum instead of kaolin, confirmed by maps showing the co-presence of Ca and S, is an interesting result that deserves to be further investigated, by analysing other Attic vases, to establish a possible connection with geographical area, furnaces, or artisan.

Author contributions

Gabriella Chirco: writing – original draft, formal analysis, investigation, visualization. Monica de Cesare: conceptualization, supervision, writing – review & editing. Giacomo Chiari: formal analysis, maps – writing – review & editing. Sarah Maaβ: formal analysis, investigation. Maria Luisa Saladino: investigation, writing – review & editing. Delia Francesca Chillura Martino: conceptualization, supervision, writing – review & editing, funding acquisition.

Conflicts of interest

There are no conflicts to declare.

Acknowledgements

Authors sincerely acknowledge the past Director, Gioconda Lamagna, of the "Pietro Griffo" Archaeological Museum in Agrigento to have granted us the possibility to study and characterize the crater. Additionally, the highly expert technical support for artefact handling by Carla Guzzone and Donatella Mangione ("Pietro Griffo" Archaeological Museum) is greatly acknowledged. Sarah Maaβ was funded for her Bachelor thesis within the student Erasmus mobility program at STEBICEF Department, Università di Palermo, Italy. We acknowledge J. Daniel Martin Ramos (Granada University) for producing the SmART_scan program. This work is part of the project PANN15T3 00384 "Scienza e archeologia: un efficace connubio per la divulgazione della cultura scientifica" granted by MIUR e.l. 113/91 (D.D. 1524/2015 – Titolo 3 – Soggetti diversi da Istituzioni Scolastiche) and of the project PON03PE 00214 2 (PON R&C 2007–2013) "Development and Application of Innovative Materials and processes for the diagnosis and restoration of Cultural Heritage – DELIAS" granted by MIUR – DD. n. 3266 del 5/12/2016. The funding source was not involved for preparation of the article, in the study design, collection, analysis and interpretation of data and in the decision to submit the article for publication.

Notes and references

1 M. de Cesare, in *Scienza e archeologia: un efficace connubio per la divulgazione della cultura scientifica*, ETS, Pisa, 2017, vol. 59–74, ISBN 978-884675210-9.
2 J. J. H. Oakley, *Picturing death in classical Athens: the evidence of the white lekythoi*, Cambridge University press, Cambridge, 2004, ISBN 8882652939.
3 J. R. Mertens, in *The Colours of Clay: Special Techniques in Athenian Vases (Exhibition, Malibu June 8-September 4, 2006)*, Getty Publications, Los Angeles, 2006, pp. 186–238, ISBN-13: 978-0-89236-942-3.
4 J. H. Oakley, in *Ta Attika. Veder greco a Gela. Ceramiche attiche figurate dall'antica colonia (Mostra, Gela, Siracusa, Rodi 2004)*, L'erma di Bretschneider, Roma, 2003, vol. 207–214, ISBN 8882652939.
5 K. Margariti, Painting early death. Deceased maidens on funerary vases in the National Archaeological Museum of Athens, *Opuscula*, 2018, **11**, 127–150, DOI: 10.30549/opathrom-11-07.
6 I. Meissner, *Weissgrundige Lekythen, Fallstudie WS2008/2009. Lehrstuhl für Restaurierung, Kunsttechnologie und Konservierungswissenschaft*, 2009, TU-München, München.
7 C. Berthold, K. B. Zimmer, O. Scharf, U. Koch-Brinkmann and K. Bente, Nondestructive, optical and X-ray analytics with high local resolution on attic white-ground lekythoi, *J. Archaeol. Sci. Rep.*, 2017, **16**, 513–520, DOI: 10.1016/j.jasrep.2016.02.008.
8 W. Noll, R. Holm and L. Born, Painting of Ancient Ceramics, *Angew. Chem., Int. Ed. Engl.*, 1975, **14**, 602–613, DOI: 10.1002/anie.197506021.
9 M. S. Walton, M. Svoboda, A. Mehta, S. Webb and K. Trentelman, Material evidence for the use of Attic white-ground lekythoi ceramics in cremation burials, *J. Archaeol. Sci.*, 2010, **37**(5), 936–940, DOI: 10.1016/j.jas.2009.11.026.
10 I. Wehgartner, presented in part at 3rd *Symposium of Ancient Greek and Related Pottery*, Copenhagen, August 31-September 4, 1987, pp. 640–651.

11 F. Caruso, in *Sicily. Art and Invention between Greece and Rome (Exhibition, Malibu, April 3-August 19, 2013)*, Getty publication, Los Angeles 2013, pp. 114–115.
12 J. D. Martin-Ramos and G. Chiari, SmART_scan : A methods to produce composition maps using any elemental molecular and image data, *J. Cult. Herit.*, 2019, **39**, 260–269, DOI: 10.1016/j.culher.2019.04.003.
13 D. Miriello, R. De Luca, A. Bloise, G. Niceforo, J. D. Martin-Ramos, A. Martellone, B. De Nigris, M. Osanna and G. Chiari, Pigments mapping on two mural paintings of the "house of garden" in Pompeii (Campania, Italy), *Mediterr. Archaeol. Archaeom.*, 2021, **21**(No 1), 257–271, DOI: 10.5281/zenodo.4574643.
14 E. Manzano, R. Blanc, J. D. Martin-Ramos, G. Chiari, P. Sarrazin and J. L. Vilchez, A combination of invasive and noninvasive techniques for the study of the palette and painting structure of a copy of Raphael's Transfiguration of Christ, *Herit. Sci.*, 2021, **9**, 150, DOI: 10.1186/s40494-021-00623-z.
15 M. C. Franceschi, E. Franceschi, D. Nole, S. Vassallo and L. Glozheni, Two Byzantine Albanian icons: a non-distractive archaeometric study, *Archaeol. Anthropol. Sci.*, 2011, **3**, 343–355, DOI: 10.1007/s12520-011-0073-0.
16 G. Chirco, E. C. Portale, E. Caponetti, V. Renda and D. Chillura Martino, Investigation on four Centuripe vases (late 3rd-2nd cent. B.C.) by portable X-ray fluorescence and total reflectance-FTIR, *J. Cult. Herit.*, 2020, **48**, 326–355, DOI: 10.1016/j.culher.2020.10.011.
17 http://schwalbe.org.chemie.uni-frankfurt.de/sites/default/files/attachments/organisch-chemisches_praktikum_i_/ir-tabellen.pdf, lastly access 22/05/21.
18 F. Rosi, A. Daveri, P. Moretti, B. G. Brunetti and C. Miliani, Interpretation of mid and near-infrared reflection properties of synthetic polymer paints for the non-invasive assessment of binding media in twentieth-century pictorial artworks, *Microchem. J.*, 2016, **124**, 898–908, DOI: 10.1016/j.microc.2015.08.019.
19 L. Fernández-Carrasco, D. Torrens-Martín, L. M. Morales and S. Martínez-Ramírez, Infrared Spectroscopy in the Analysis of Building and Construction Materials, *Infrared Spectroscopy – Materials Science, Engineering and Technology*, 2012, pp. 369–384. DOI: 10.5772/36186.
20 J. L. Bishop, M. D. Lane, M. D. Dyar, S. J. King, A. J. Brown and G. A. Swayze, Spectral properties of Ca-Sulfates: gypsum, Bassanite and Anhydrite, *Am. Mineral.*, 2014, 2105–2115, DOI: 10.2138/am-2014-4756.
21 http://lisa.chem.ut.ee/IR_spectra/, accessed 12.05.21.
22 J. Ouyang, D. Mu, Y. Zhang and H. Yang, Mineralogy and Physico-Chemical Data of Two Newly Discovered Halloysite in China and Their Contrasts with Some Typical Minerals, *Minerals*, 2018, **8**(3), 108, DOI: 10.3390/min8030108.
23 T. Sievert, A. Wolter and N. B. Singh, Hydration of anhydrite of gypsum (CaSO4.II) in a ball mill, *Cem. Concr. Res.*, 2005, **35**, 623–630, DOI: 10.1016/j.cemconres.2004.02.010.
24 E. Murad and U. Wagner, Clays and clay minerals: The firing process, *Hyperfine Interact.*, 1998, **117**, 337–356, DOI: 10.1023/a:1012683008035.
25 M. Trindade, M. Dias, J. Coroado and F. Rocha, Mineralogical transformations of calcareous rich clays with firing: A comparative study between calcite and dolomite rich clays from Algarve, Portugal, *Appl. Clay Sci.*, 2009, **42**, 345–355, DOI: 10.1016/j.clay.2008.02.008.
26 R. F. Conley and W. M. Bundy, Mechanism of gypsification, *Geochim. Cosmochim. Acta*, 1958, **15**, 57–72.
27 S. Shoval, Using FT-IR spectroscopy for study of calcareous ancient ceramics, *Opt. Mater.*, 2003, **24**, 117–122, DOI: 10.1016/S0925-3467(03)00114-9.
28 L. Pappalardo, S. Barresi, G. Biondi, C. Caliri, F. Caruso, R. Catalano, G. Lamagna, G. A. Manenti, G. Monterosso, A. Orlando, F. Rizzo, F. P. Romano and H. C. Santos, PIXE-alpha non-destructive and in situ compositional investigation of black gloss on ancient pottery: Non-destructive and in situ PIXE-alpha analysis on ancient black gloss, *X-Ray Spectrom.*, 2016, **45**, 258–262, DOI: 10.1002/xrs.2696.
29 L. J. Janik and J. L. Keeling, *Quantitative determination of halloysite using FT-IR PLS analysis and its application to the characterization of kaolins from north-western Eyre Peninsula, South Australia*, Division of Soils Divisional Report, vol. 129, 1996, ISBN: 0643058664.
30 M. Yang, M. Ye, H. Han, G. Ren, L. Han and Z. Zhang, Near-Infrared Spectroscopic Study of Chlorite Minerals, *J. Spectrosc.*, 2018, **1**, 1–11, DOI: 10.1155/2018/6958260.
31 M. Vidale in *Ceramica e Archeologia*, Carocci editore, Roma, 2007, vol. 10–19, ISBN: 9788843042814.
32 M. E. Ouahabi, L. Daoudi, F. Hatert and N. Fagel, Modified Mineral Phases During Clay Ceramic Firing, *Clays Clay Miner.*, 2015, **63**, 404–413, DOI: 10.1346/ccmn.2015.0630506344-4.
33 M. A. Mastelloni, *Lipára ed il teatro in età tardoclassica ed ellenistica*, Liriti Editore, Regio Calabria, 2015, ISBN 978-88-6164.
34 A. M. W. Hunt and R. J. Speakman, Portable XRF analysis of archaeological sediments and ceramics, *J. Archaeol. Sci.*, 2015, **53**, 626–638, DOI: 10.1016/j.jas.2014.11.031.
35 M. L. Saladino, S. Ridolfi, I. Carocci, G. Chirco, S. Caramanna and E. Caponetti, A multi-disciplinary investigation of the "Tavolette fuori posto" of the "Hall of Barons" wooden ceiling of the "Steri" (Palermo, Italy), *Microchem. J.*, 2016, **126**, 132–137, DOI: 10.1016/j.microc.2015.12.004.
36 G. Testa and S. Lugli, Gypsum–anhydrite transformations in Messinian evaporites of central Tuscany (Italy), *Sediment. Geol.*, 2000, **130**, 249–268, DOI: 10.1016/S0037-0738(99)00118-9.
37 M. F. Alberghina, S. Schiavone, C. Greco, M. L. Saladino, F. Armetta, V. Renda and E. Caponetti, How many secrets details a systematic multi-analytical study could still reveal about the mysterious fresco Trionfo della Morte in Palermo?, *Heritage*, 2019, **2**(3), 2370–2383, DOI: 10.3390/heritage2030145.
38 P. S. R. Prasad, V. Krishna Chaitanya, K. Shiva Prasad and D. Narayana Rao, Direct formation of the γ-$CaSO_4$ phase in

dehydration process of gypsum: In situ FTIR study, *Am. Mineral.*, 2005, **90**(10), 672–678, DOI: 10.2138/am.2005.1742.

39 J. M. Perez and R. Esteve-Tebar, Pigment identification in Greek pottery by Raman microspectroscopy, *Archaeometry*, 2004, **46**, 607–614, DOI: 10.1111/j.1475-4754.2004.00176.x.

40 F. Cavari in *Introduzione allo studio della ceramica in archeologia*, Centro Editoriale Toscano sas, Firenze 2007, pp. 63–86, ISBN 10: 88-7957-269-5.

41 H. G. Dill, F. Melcher and S. Kaufhold, Post-Miocene and bronze age supergene Cu–Pb arsenate – Humate – oxalate – carbonate mineralization at Mega Liavadi, Serifos, Greece, *Can. Mineral.*, 2010, **48**, 163–181, DOI: 10.3749/canmin.48.1.163.

42 G. Biondi and F. P. Romano, Un nuovo vaso policromo e riflessioni sull'iconografia delle scene sui vasi di Centuripe, *Bulletin Antieke Beschaving*, 2018, **93**, 105–129, DOI: 10.2143/bab.93.0.3284848.